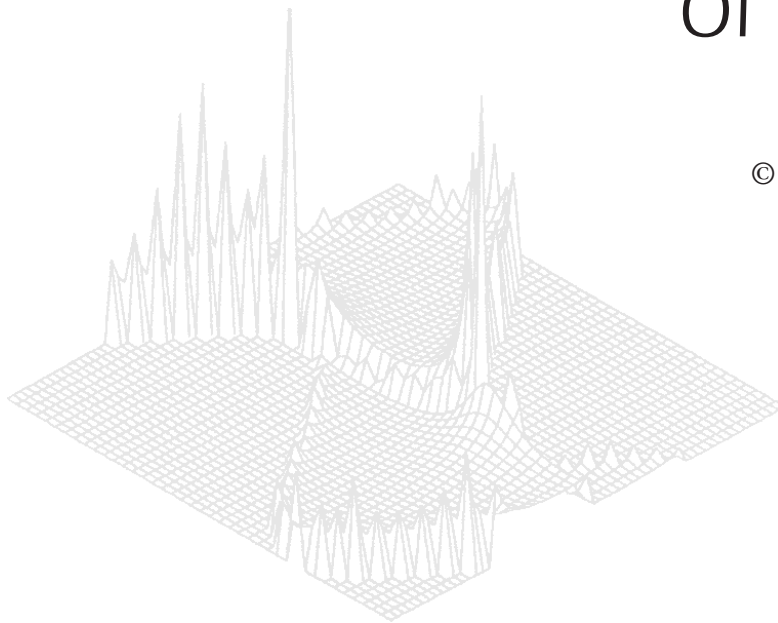

C S I R O P U B L I S H I N G

Australian Journal of Physics

Volume 52, 1999
© CSIRO Australia 1999



A journal for the publication of
original research in all branches of physics

www.publish.csiro.au/journals/ajp

All enquiries and manuscripts should be directed to

Australian Journal of Physics

CSIRO PUBLISHING

PO Box 1139 (150 Oxford St)

Collingwood

Vic. 3066

Australia

Telephone: 61 3 9662 7626

Facsimile: 61 3 9662 7611

Email: peter.robertson@publish.csiro.au



Published by **CSIRO PUBLISHING**
for CSIRO Australia and
the Australian Academy of Science



Electron Scattering from the Ground and Excited States of Barium*

Dmitry V. Fursa

School of Physical Sciences, Flinders University of South Australia,
GPO Box 2100, Adelaide, SA 5001, Australia.
email: Dmitry.Fursa@flinders.edu.au

Abstract

We have used the nonrelativistic convergent close-coupling (CCC) method to investigate electron scattering from the ground $(6s^2)^1S$ state and excited $(6s6p)^1P_1^o$ and $(6s5d)^1,^3D_2^o$ states of barium. For the scattering from the barium ground state, we have found very good agreement with measurements of $(6s6p)^1P_1^o$ apparent cross sections at all energies. Similarly, good agreement is found for differential cross sections for elastic scattering and $(6s6p)^1P_1^o$ and $(6s5d)^1D_2^o$ excitations and with the $(6s6p)^1P_1^o$ state electron–photon angular correlations. For the scattering from excited states of barium we have found good agreement with elastic $(6s6p)^1P_1^o$ scattering and the $(6s5d)^1D_2^o \rightarrow (6s6p)^1P_1^o$ transition for both differential cross sections and electron–photon angular correlations.

1. Introduction

Significant progress has been achieved over the last few years in our understanding of electron scattering from the barium atom. From the experimental side, this progress is related to new detailed measurements of electron scattering from the laser-excited $(6s6p)^1P_1^o$ state and metastable $(6s5d)^1,^3D_2^o$ states. On the theoretical side, the convergent close-coupling method (CCC) has been used to perform the first large scale close-coupling calculations over a wide range of incident electron energies and scattering processes.

Experimental study of electron–barium scattering has been a subject of considerable interest over the last few decades. To date, a large amount of accurate experimental data has been accumulated for scattering from the ground state of the barium atom. These data include the measurements of the $(6s6p)^1P_1^o$ apparent cross section (Chen and Gallagher 1976), the total ionisation cross section (Dettmann and Karstensen 1982), the total cross section (Romanyuk *et al.* 1980), and the differential cross sections for elastic scattering and excitations of the $(6s6p)^1P_1^o$ and $(6s5d)^1D_2^o$ states (Jensen *et al.* 1978; Wang *et al.* 1994).

These earlier experimental data for the scattering from the barium ground state have been recently complemented by the study of electron scattering from barium excited states. The availability of the latter data is due to a particularly

* Refereed paper based on a contribution to the Australia–Germany Workshop on Electron Correlations held in Fremantle, Western Australia, on 1–6 October 1998.

useful feature of the barium atom, which is the possibility to use readily available lasers in order to prepare a large population of the $(6s6p)^1P_1^o$ level. Superelastic scattering from the laser-prepared $(6s6p)^1P_1^o$ level has been studied by Zetner *et al.* (1992, 1993) and Li and Zetner (1994), who determined electron-impact coherence parameters (EICPs) for the time ‘inverse’ $(6s6p)^1P_1^o-(6s^2)^1S$ transition. Similar experimental techniques have been used to measure the differential cross section and EICPs for elastic scattering from the laser prepared $(6s6p)^1P_1^o$ level by Trajmar *et al.* (1998) and for the $(6s6p)^1P_1^o-(6s5d)^1D_2^e$ transition by Li and Zetner (1995). In addition, differential cross sections have been measured for the excitation of a number of barium levels from the $(6s6p)^1P_1^o$ level by Zetner *et al.* (1997) and for scattering from the cascade-populated metastable $(6s5d)^{1,3}D_2^e$ levels by Zetner *et al.* (1999).

It has been the aim of the atomic theory group at Flinders University to provide theoretical support for the experimental e–Ba scattering program. We have used the CCC method to calculate electron scattering from barium ground and excited states. The CCC method was originally developed for the calculation of electron scattering from the hydrogen atom (Bray and Stelbovics 1992). It was later generalised to the calculation of electron scattering from quasi-one-electron targets (Li, Na) (Karaganov *et al.* 1996; Bray 1994), helium (Fursa and Bray 1995) and beryllium (Fursa and Bray 1997) with considerable success.

While former applications of the CCC method were limited to light atoms, the present study of electron scattering from barium allows us to test the CCC method for the new set of target atoms, heavy atoms. The choice of the barium atom was dictated by the prior availability of accurate experimental data and ongoing experimental interest in e–Ba scattering. Another reason to apply the CCC method to the e–Ba scattering problem has been a failure of the earlier theoretical methods to describe a substantial portion of the experimental data (see Fursa and Bray 1999 for a detailed comparison).

It is well known that the nonrelativistic approximation breaks down for heavy targets. Application of the CCC method, in its present nonrelativistic formulation, therefore, requires additional considerations. It was found in a number of earlier publications (Trefftz 1974; Rose *et al.* 1978; Bauschlicher *et al.* 1985) that the spin–orbit coupling leads to a substantial singlet–triplet mixing in the barium spectrum. However, it was also found that relativistic effects are not important for the description of the barium states included in the present study (Clark *et al.* 1989; Srivastava *et al.* 1992*b*; Zetner *et al.* 1997). The singlet–triplet mixing affects most scattering cross sections for weak transitions. These are transitions which in the nonrelativistic approximation can happen only due to the exchange scattering. In this case even a small admixture of the direct channel can substantially change the results (Fursa and Bray 1999). In the present paper we have presented results only for spin-preserving transitions which are not affected by the breaking down of the nonrelativistic approximation.

The plan of the paper is as follows. We give a short summary of the CCC method and its application to the e–Ba scattering problem in Section 2. Then, in Section 3, we provide the relevant theoretical formalism required to compare our theoretical calculations with experimental results obtained from electron scattering from laser-prepared states of barium. We compare results of our calculations with experiment in Section 4 and, finally, formulate conclusions in Section 5.

2. Barium Structure and Electron–Barium Scattering

The details of the CCC theory for electron scattering from alkaline-earth atoms have been given by Fursa and Bray (1997) and specific application to electron–barium scattering has been discussed by Fursa and Bray (1999). Here we give a short summary of the CCC method.

The CCC method is formulated in the nonrelativistic approximation, for both structure and scattering calculations. The Russell–Saunders coupling scheme (*LS* scheme) is adopted for the description of barium atom wave functions and for the total (projectile and target electrons) wave function.

The barium wave functions are described by a model with two valence electrons above the inert Hartree–Fock core. The Hamiltonian of the barium atom can be written as

$$H_{\text{T}} = H_1 + H_2 + V_{12}, \quad (1)$$

where H_i , $i = 1, 2$ is the one-electron Hamiltonian,

$$H_i = -\frac{1}{2}\nabla_i^2 + V_i^{\text{FC}} + V_i^{\text{pol}}. \quad (2)$$

The frozen-core Hartree–Fock potential V^{FC} is obtained from a self-consistent-field Hartree–Fock calculation for the ground state of the Ba^+ ion and the phenomenological polarisation potential V^{pol} is given by

$$V^{\text{pol}}(r) = -\frac{\alpha_d}{2r^4} W_6(r/\rho), \quad (3)$$

where

$$W_m(r/\rho) = \{1 - \exp[-(r/\rho)^m]\}, \quad (4)$$

and $\alpha_d = 11$ a.u. is the static dipole polarisability of the Ba^+ core.

The two-electron potential V_{12} is a modified electron–electron potential,

$$V_{12}(\hat{\mathbf{r}}_1 \cdot \hat{\mathbf{r}}_2) = 1/|r_1 - r_2| + V_{12}^{\text{di-el}}(\hat{\mathbf{r}}_1 \cdot \hat{\mathbf{r}}_2), \quad (5)$$

where $V^{\text{di-el}}$ is the phenomenological two-electron polarisation potential,

$$\begin{aligned} V_{12}^{\text{di-el}}(\hat{\mathbf{r}}_1 \cdot \hat{\mathbf{r}}_2) &= -\frac{\alpha_d}{r_1^2 r_2^2} P_1(\hat{\mathbf{r}}_1 \cdot \hat{\mathbf{r}}_2) \sqrt{W_6(r_1/\rho) W_6(r_2/\rho)} \\ &= W^{\text{d}}(r_1, r_2) P_1(\hat{\mathbf{r}}_1 \cdot \hat{\mathbf{r}}_2), \end{aligned} \quad (6)$$

and P_1 is the Legendre polynomial of degree 1.

We obtain one-electron functions by diagonalising the one electron Hamiltonian (2) in a large basis of Sturmian (Laguerre) functions. The parameter ρ in (3) has been chosen to fit the low-lying energy spectrum of the Ba^+ ion for each value l of the orbital angular momentum. In the present calculations we construct the *s*, *p*, *d* and *f* one electron functions. The orthonormal one-electron basis obtained this way is complete and square-integrable. It is used to perform standard configuration-interaction calculations for the barium atom. This is

done by constructing a set of two-electron functions (configuration set) and diagonalising the Hamiltonian (1) of the barium atom in this set. The parameter ρ in the phenomenological two-electron polarisation potential (6) has been chosen to obtain the best agreement with the ionisation energies of the $(6s6p)^1P_1^o$ and $(6s5d)^1D_2^o$ states

We have chosen the configuration set in such a way that one of the electrons always occupies one of the $6s$, $7s$, $6p$, $7p$ or $5d$ orbitals of the Ba^+ ion. This set has proved to be wide enough to allow for a sufficiently accurate description of the negative energy (relative to the Ba^+ ground state) spectrum of the barium atom—see Fursa and Bray (1999) for details. It also allows us to avoid very fine discretisation of the barium atom continuum spectrum which makes it possible to account for coupling to ionisation channels in the consequent close-coupling calculations.

The resulting target states Φ_n of the barium atom satisfy

$$\langle \Phi_{n'} | H_T | \Phi_n \rangle = \epsilon_n \delta_{n'n}, \quad n = 1, \dots, N, \quad (7)$$

where ϵ_n is the energy associated with Φ_n and N is the number of the barium target states.

We use barium target states Φ_n in order to perform a multichannel expansion of the total (projectile and target electrons) wave function $\Psi^{(+)}$ with outgoing spherical wave boundary conditions,

$$|\Psi^{(+)}\rangle = (1 - P_{rs}) \sum_{n=1}^N |\Phi_n\rangle \langle \Phi_n | \psi_i^{(+)}\rangle, \quad (8)$$

where the space and spin exchange operator P_{rs} ensures the antisymmetry of the total wave function and allows us to work with a nonsymmetrised function $\psi_i^{(+)}$. The scattering information is obtained from the calculation of the T matrix defined as

$$\langle \mathbf{k}_f \Phi_f | T^N | \mathbf{k}_i \Phi_i \rangle = \langle \mathbf{k}_f \Phi_f | (H - E) | \Psi^{(+)} \rangle, \quad (9)$$

where $|\mathbf{k}\rangle$ is a plane wave, and H and E are the total Hamiltonian and energy of the scattering system, respectively. The index N on the T matrix indicates the approximation of including only N states in the close-coupling expansion (8).

In order to find the T -matrix we solve the coupled Lippmann–Schwinger equations in momentum space,

$$\begin{aligned} \langle \mathbf{k}_f \Phi_f | T^N | \Phi_i \mathbf{k}_i \rangle &= \langle \mathbf{k}_f \Phi_f | V | \Phi_i \mathbf{k}_i \rangle \\ &+ \sum_{n=1}^N \int \mathbf{k} \frac{\langle \mathbf{k}_f \Phi_f | V | \Phi_n \mathbf{k} \rangle \langle \mathbf{k} \Phi_n | T^N | \Phi_i \mathbf{k}_i \rangle}{E^{(+)} - \epsilon_k - \epsilon_n}, \end{aligned} \quad (10)$$

where $V = H - H_T - K_0 - (H - E)P_{rs}$, and K_0 is the projectile kinetic energy operator.

The present calculations have been performed in two models. First, we have included only negative energy states in the close-coupling expansion. This calculation comprises 55 states: five 1S , six $^1P^o$, seven $^1D^e$, five $^1F^o$, three 3S , six $^3P^o$, five $^3D^e$, five $^3F^o$, one $^1P^e$, three $^1D^o$, one $^1F^e$, three $^3P^e$, three $^3D^o$, and two $^3F^e$ states. Second, we have performed 115-state calculations which include both negative- and positive-energy states: 14 1S , 17 $^1P^o$, 19 $^1D^e$, 19 $^1F^o$, 7 3S , 9 $^3P^o$, 9 $^3D^e$, 9 $^3F^o$, and two each of $^1,3P^e$, $^1,3D^o$, $^1,3F^e$ states. The difference between results of the two models will give an estimate of the influence of the coupling to the target ionisation continuum on the scattering results. We have performed CC(55) calculations over a wide range of incident electron energies (1–987 eV). The CCC(115) calculations have been performed at the selected energy points in order to estimate the effect of the coupling to the target ionisation continuum. The choice of these points was dictated by the availability of detailed experimental data.

3. Measurement Theory

In this section we would like to present the theoretical formalism required to relate the scattering amplitudes calculated in the CCC method to the recent measurements of differential cross sections and electron-impact coherence parameters for scattering from the laser excited $6s6p^1P_1^o$ level of the barium atom (Johnson *et al.* 1999; Trajmar *et al.* 1998).

The collision frame scattering amplitude for the transition from initial state Φ_i with angular momentum J_i and magnetic sublevel M_i to final state Φ_f with angular momentum J_f and magnetic sublevel M_f is

$$f_{J_f M_f, J_i M_i}(m_f, m_i) = \langle \mathbf{k}_f \Phi_f | T^N | \Phi_i \mathbf{k}_i \rangle, \quad (11)$$

where m_f and m_i are projectile electron initial and final spin projections. The dependence of the scattering amplitudes on the spherical polar angles θ and φ of the detected electron is implicit.

In the case of electron impact from the isotropic populated initial state Φ_i , the differential cross section for the excitation of the state Φ_f is given by

$$\text{DCS} = \frac{k_f}{2(2J_i + 1)k_i} \sum_{M_f, M_i, m_f, m_i} |f_{J_f M_f, J_i M_i}(m_f, m_i)|^2. \quad (12)$$

The summation in equation (12) over projectile electron initial and final spin projection m_i and m_f indicates that no electron spin analysis is performed.

We now turn to the scattering from the laser-excited state Φ_i (with anisotropic population of the magnetic sublevels). The description of the laser-excited state of barium, in terms of the density matrix or, equivalently, state multipoles, is simpler not in the collision frame but in the photon frame (Macek and Hertel 1974). We follow the definitions given by Zetner *et al.* (1990). The laser beam incident direction is specified by the spherical polar angles θ_ν and φ_ν with respect to the collision frame. Two cases should be considered separately: laser-pumping with circular and linear polarised light.

For the circular polarised light the photon frame quantisation axis is chosen antiparallel to the laser beam incident direction. The photon frame can be

obtained from the collision frame through rotations by Euler angles $\alpha = \varphi_\nu$, $\beta = \theta_\nu - \pi$ and $\gamma = 0$ (we use the same definition of the Euler angles as in Edmonds 1957). The state multipoles $\tilde{T}_{kq}^{(a)}$ of the barium atom P-state in the photon frame are

$$\tilde{T}_{kq}^{(a)} = \delta_{q,0} C_{1\mp 1,1\pm 1}^{k0} : \tilde{T}_{00}^{(a)} = \sqrt{\frac{1}{3}}, \tilde{T}_{10}^{(a)} = \mp \sqrt{\frac{1}{2}}, \tilde{T}_{20}^{(a)} = \sqrt{\frac{1}{6}}, \quad (13)$$

where \mp refers to right and left circular polarisation. In the collision frame they are given by

$$T_{kq}^{(a)} = \tilde{T}_{k0}^{(a)} D_{q0}^k(\varphi_\nu, \theta_\nu - \pi, 0). \quad (14)$$

For linear polarised light the photon frame is chosen along the polarisation vector. This photon frame can be obtained from the photon frame for the circular polarised light through rotations by Euler angles $\alpha = \psi$, $\beta = \pi/2$, and $\gamma = 0$, where ψ is the angle between the polarisation vector and the X -axis of the photon frame for the circular polarised light. In this case the state multipoles are

$$\tilde{T}_{kq}^{(a)} = -\delta_{q,0} C_{10,k0}^{10} : \tilde{T}_{00}^{(a)} = \sqrt{\frac{1}{3}}, \tilde{T}_{10}^{(a)} = 0, \tilde{T}_{20}^{(a)} = -\sqrt{\frac{2}{3}}. \quad (15)$$

In the collision frame they are given by

$$T_{kq}^{(a)} = \sum_{\mu} \tilde{T}_{k0}^{(a)} D_{q\mu}^k(\varphi_\nu, \theta_\nu - \pi, 0) D_{\mu 0}^k(\psi, \pi/2, 0). \quad (16)$$

The differential cross section for scattering from the laser excited state (PDCS) can be found from (Macek and Hertel 1974)

$$\text{PDCS} = \frac{\text{DCS}}{T_{00} T_{00}^{(a)}} \sum_{kq} T_{kq} T_{kq}^{(a)}. \quad (17)$$

Here the state multipoles T_{kq} are given by

$$T_{kq} = \sum_{M, M'} (-1)^{J_i - M'} C_{J_i M J_i - M'}^{kq} \rho_{MM'}, \quad (18)$$

where the density matrix is

$$\rho_{M_i M'_i} =$$

$$\sum_{M_f, m_f, m_i} f_{J M_f, J_i M'_i}(m_f, m_i) f_{J M_f, J_i M_i}^*(m_f, m_i) \bigg/ \sum_{M, M', m, m'} |f_{J M', J_i M}(m', m)|^2. \quad (19)$$

The density matrix is normalised to unit trace, $\text{tr}\rho = 1$, and the state multipoles are normalised to have $T_{00} = 1/\sqrt{2J_i + 1}$.

For circular polarised light we obtain from (14) and (17)

$$\begin{aligned} \text{PDCS}_{\text{LHS}}^{\text{RHS}}(\theta_\nu, \varphi_\nu) &= \frac{\text{DCS}}{T_{00}T_{00}^{(a)}} [T_{00}T_{00}^{(a)} \pm \sqrt{2}i|T_{11}|\tilde{T}_{10}^{(a)} \sin\theta_\nu \sin\varphi_\nu \\ &\quad + \tilde{T}_{20}^{(a)} \sqrt{\frac{3}{2}}(T_{22} \sin\theta_\nu \cos 2\varphi_\nu - T_{21} \sin 2\theta_\nu \cos\varphi_\nu \\ &\quad + T_{20} \sqrt{\frac{1}{6}}(3 \cos^2\theta_\nu - 1))] , \end{aligned} \quad (20)$$

where the RHS (LHS) subscript indicates right-hand (left-hand) circularly polarised light.

For the linear polarised light we obtain from (16) and (17)

$$\begin{aligned} \text{PDCS}(\theta_\nu, \varphi_\nu, \psi) &= \frac{\text{DCS}}{T_{00}T_{00}^{(a)}} [T_{00}T_{00}^{(a)} + \tilde{T}_{20}^{(a)} \sqrt{\frac{3}{8}}\{T_{22}((1 + \cos^2\theta_\nu) \cos 2\varphi_\nu \cos 2\psi \\ &\quad + 2 \cos\theta_\nu \sin 2\varphi_\nu \sin 2\psi - \sin^2\theta_\nu \cos 2\varphi_\nu) \\ &\quad + T_{21}(\sin 2\theta_\nu \cos\varphi_\nu \\ &\quad + \sin 2\theta_\nu \cos\varphi_\nu \cos 2\psi + 2 \sin 2\theta_\nu \sin\varphi_\nu \sin 2\psi) \\ &\quad + T_{20} \sqrt{\frac{2}{3}}(3 \sin^2\theta_\nu \cos^2\psi - 1)\}] . \end{aligned} \quad (21)$$

Zetner *et al.* (1997) have measured the differential cross section for the barium P-state pumped with linearly polarised laser light propagating in the scattering plane ($\varphi = 0^\circ$ or 180°). In this case equation (21) can be written as

$$\begin{aligned} \text{PDCS}_\pm(\theta_\nu, \psi) &= \frac{\text{DCS}}{T_{00}T_{00}^{(a)}} [T_{00}T_{00}^{(a)} + \tilde{T}_{20}^{(a)} \sqrt{\frac{3}{2}}(T_{22}(\cos^2\theta_\nu \cos^2\psi - \sin^2\psi) \\ &\quad \pm T_{21} \sin 2\theta_\nu \cos^2\psi + T_{20} \sqrt{\frac{1}{6}}(3 \sin^2\theta_\nu \cos^2\psi - 1))] , \end{aligned} \quad (22)$$

where the positive sign corresponds to $\varphi = 0^\circ$ and negative to $\varphi = 180^\circ$. An interesting feature of the last equation, noted by Zetner *et al.* (1997), is that the special choice of the angles $\theta_\nu = 45^\circ$ and $\psi = 35.3^\circ$ ($\cos^2\psi = \frac{2}{3}$) makes coefficients of state multipoles T_{20} and T_{22} equal to zero. Therefore, one can determine the differential cross section for scattering from an unpolarised target from the measurements of the PDCS_\pm ,

$$\text{DCS} = \frac{1}{2}[\text{PDCS}_+(45^\circ, 35.3^\circ) + (\text{PDCS}_-(45^\circ, 35.3^\circ))] . \quad (23)$$

The density matrix $\rho_{M_i M'_i}$ and state multipoles T_{kq} allow for a different interpretation which is related to the ‘inverse’ scattering process. In this process the electron scattering from the isotropic Φ_f state results in the excitation of the Φ_i state which is described by the density matrix $\rho_{MM'}$ and state multipoles T_{kq} . The quantisation axis for the ‘inverse’ scattering process is chosen antiparallel to the scattered electron momentum vector \mathbf{k}_f . If the laser beam incident direction is measured with respect to this new quantisation axis then equations (20) and (21) for the measured scattering intensity stay exactly the same.

The state multipoles T_{kq} describe alignment and orientation of the Φ_i state and can be determined from the measurements of the PDCS. Such measurements have been performed for the $6s6s^1S \rightarrow 6s6p^1P_1^o$ transition by Zetner *et al.* (1992, 1993) and Li and Zetner (1994), for the $6s5d^1D_2^e \rightarrow 6s6p^1P_1^o$ transition by Johnson *et al.* (1999), and for the $6s6p^1P_1^o \rightarrow 6s6p^1P_1^o$ transition by Trajmar *et al.* (1998). The experimental measurements for the two former transitions involved determination of the parameters P_1 , P_2 , P_3 which coincide with the Stokes parameters measured in polarisation-correlation electron–photon coincidence experiments,

$$P_1 = \frac{\text{PDCS}(90^\circ, 90^\circ, 0^\circ) - \text{PDCS}(90^\circ, 90^\circ, 90^\circ)}{\text{PDCS}(90^\circ, 90^\circ, 0^\circ) + \text{PDCS}(90^\circ, 90^\circ, 90^\circ)}, \quad (24)$$

$$P_2 = \frac{\text{PDCS}(90^\circ, 90^\circ, 45^\circ) - \text{PDCS}(90^\circ, 90^\circ, 135^\circ)}{\text{PDCS}(90^\circ, 90^\circ, 45^\circ) + \text{PDCS}(90^\circ, 90^\circ, 135^\circ)}, \quad (25)$$

$$P_3 = \frac{\text{PDCS}_{\text{RHS}}(90^\circ, 90^\circ) - \text{PDCS}_{\text{LHS}}(90^\circ, 90^\circ)}{\text{PDCS}_{\text{RHS}}(90^\circ, 90^\circ) + \text{PDCS}_{\text{LHS}}(90^\circ, 90^\circ)}. \quad (26)$$

For the excitation of the $6s6p^1P_1^o$ state from the barium ground state the determination of the Stokes parameters and differential cross section allows for the complete description of the scattering process, see Andersen *et al.* (1998) for a detailed discussion. However, for scattering from both $6s5d^1D_2^e$ and $6s6p^1P_1^o$ states the complete experiment is not possible, though one can determine all (five) nonzero state multipoles T_{kq} . This can be achieved by making additional measurements, i.e. of the parameter λ ,

$$\lambda = \rho_{00} = \frac{\text{PDCS}(90^\circ, 45^\circ, 0^\circ)}{\text{PDCS}(90^\circ, 45^\circ, 0^\circ) + \text{PDCS}(90^\circ, 45^\circ, 90^\circ)}. \quad (27)$$

These measurements have been performed for the $6s5d^1D_2^e \rightarrow 6s6p^1P_1^o$ transition (Johnson *et al.* 1999).

Measurements for the elastic scattering from the $6s6p^1P_1^o$ state involved laser pumping with linear polarised light propagating in the scattering plane (Trajmar *et al.* 1998). The scattering intensity in this case can be written in the form of a modulation equation,

$$\text{DCS}^{el} = \frac{3}{4} \text{DCS}(A + B \cos 2\psi), \quad (28)$$

where the coefficients A and B are functions of the state multipoles T_{kq} or, alternatively, can be expressed via the electron-impact coherence parameters $[\lambda, \cos \varepsilon, k = 2\sqrt{\lambda(1-\lambda)} \cos \delta \cos \tilde{\chi}]$ as defined by da Paixão *et al.* (1980). The values of coefficients A and B have been obtained for a number of laser orientations from least-squares fitting of measured scattering intensity. This, in turn, allowed the determination of the EICPs λ , $\cos \varepsilon$ and k —see Trajmar *et al.* (1999) for a detailed discussion.

We would like to make a few notes on the scattering from the metastable $6s5d^{1,3}D_2$ levels. These levels are populated by the cascade radiation from the laser-pumped $6s6p^1P_1^o$ level. Bizzarri and Huber (1990) have measured the branching fractions for the $6s6p^1P_1^o$ level radiative decay which indicates that the cascade to the $6s5d^3D_1$ level is negligible. Note that a cascade from a singlet P-level to a triplet $D_{1,2}$ levels suggests a breakdown of the nonrelativistic approximation for the barium atom.

The theoretical formalism presented above is made specific to the laser excited barium $6s6p^1P_1^o$ state only via the photon frame state multipoles $\tilde{T}_{kq}^{(a)}$. We can, therefore, consider scattering from the metastable $6s5d^{1,3}D_2$ levels using exactly the same formalism provided the corresponding photon-frame state multipoles are known. The only required modification to the above expressions is the replacement of the $\tilde{T}_{kq}^{(a)}$ for the $6s6p^1P_1^o$ state with those of the cascade-populated metastable levels. The latter can be found from the following relation:

$$\tilde{T}_{kq}^{(a)}(6s5d^{1,3}D_2^e) = \beta_k \tilde{T}_{kq}^{(a)}(6s6p^1P_1^o), \quad (29)$$

where

$$\beta_0 = \sqrt{3/5}, \quad \beta_1 = 3\sqrt{5}/10, \quad \beta_2 = \sqrt{21}/10. \quad (30)$$

Equation (29) relates the state multipoles of the $6s6p^1P_1^o$ state and the state multipole of the cascade-populated $6s5d^{1,3}D_2$ state provided that polarisation and angular distribution of the dipole radiation are not registered. We refer to Korenman (1975) for the details. Note that coefficients $\beta_k/\beta_0 < 1$ and, therefore, the anisotropic population of the metastable states is relatively smaller than the original $6s6p^1P_1^o$ state. This might result in a relatively weaker sensitivity of the measured scattering intensity to the variation of the laser incident direction and polarisation vector.

In the same way as it has been done for the $6s6p^1P_1^o$ state, measurements of scattering intensities corresponding to electron scattering from the anisotropic metastable states can be performed. The Stokes parameters and EICPs which describe alignment and orientation of the metastable states atomic charge cloud for the ‘inverse’ scattering process can be determined from those measurements. The unusual feature of such experiment is the absence of the counterpart electron–photon coincidence experiment because the $6s5d^{1,3}D_2$ state cannot decay to the barium ground state by emitting a dipole photon.

4. Results

In this section we compare results of the CCC calculations with experimental data. We start with testing the applicability of the CCC method to e–Ba scattering

by comparing with the accurate experimental data available for scattering from the barium ground state (see Fursa and Bray 1999 for a detailed comparison). Good agreement with these data would be a solid foundation for analysing experimental data for electron scattering from excited states.

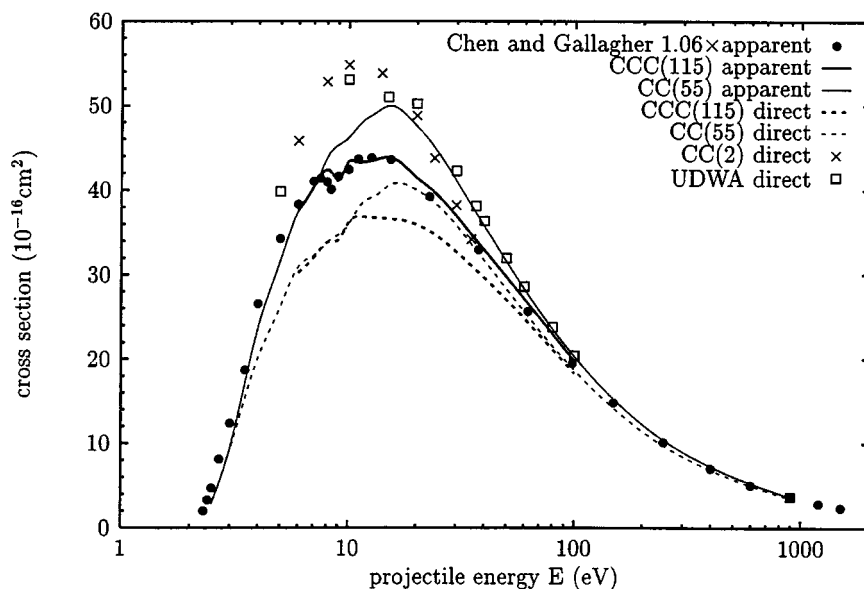


Fig. 1. Apparent and direct $6s6p^1P_1^o$ excitation integrated cross sections for electron scattering from the Ba ground state. The CCC(115) and CC(55) calculations are described in the text. The UDWA calculations are due to Clark *et al.* (1989) and CC(2) calculations are due to Fabrikant (1980). The experiment by Chen and Gallagher (1976) has been renormalised by a factor of 1.06 (see text).

One of the most important experimental studies in e–Ba scattering was the measurement of the optical excitation function for the resonance transition in barium by Chen and Gallagher (1976). The optical excitation function is a sum of the direct excitation integrated cross section (ICS) of the $(6s6p)^1P_1^o$ level and the cascade contribution from the higher-lying levels. High accuracy of the experimental data of Chen and Gallagher (1976) allows us to perform a severe test of the theoretical methods. In Fig. 1 we present results of our CCC(115) and CC(55) calculations for the direct $(6s6p)^1P_1^o$ ICS and for the apparent cross section (direct plus cascades). We have also presented results of the two-state close-coupling calculations of Fabrikant (1980) and the UDWA calculations of Clark *et al.* (1989) for the direct ICS. We can see that both latter calculations substantially overestimate the experimental data. The inclusion of the cascades in those calculations would further increase the discrepancy. On other hand, both CCC(115) and CC(55) direct ICS are below the experimental data. However, when the cascade contribution is added, we find that the CC(55) apparent cross section overestimates the experimental data, while CCC(115) results are in quantitative agreement with the experimental data. The difference between CCC(115) and CC(55) apparent cross sections is an indication of the importance

of the coupling to the ionisation channels, which was crucial in this case in order to achieve agreement with the experimental data. Note that experimental data in Fig. 1 have been multiplied by a factor of 1.06 in order to account for more accurate higher energy normalisation.

In Fig. 2 we present a comparison between theoretical calculations and measurements of the differential cross sections (DCS) for the elastic scattering

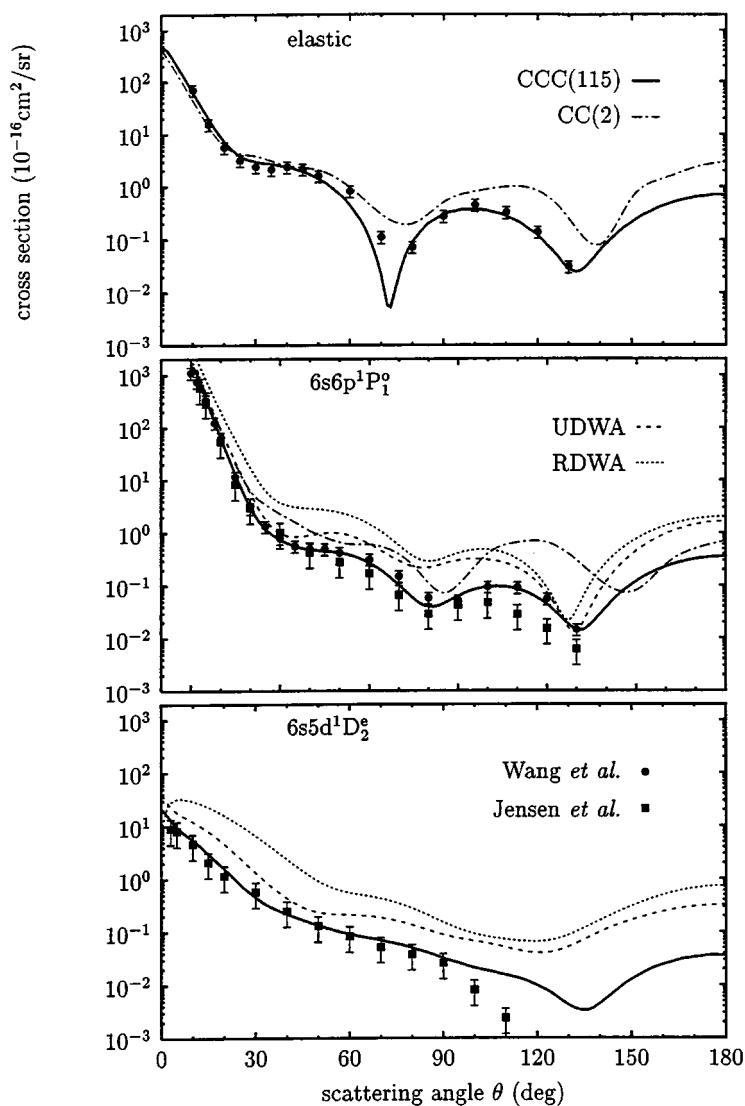


Fig. 2. Elastic, $6s6p^1P_1^o$ and $6s5d^1D_2^e$ excitation differential cross sections for electron scattering from the Ba ground state at 20 eV incident electron energy. The CCC(115) calculation is described in the text. The UDWA calculations are due to Clark *et al.* (1989), the RDWA calculations are due to Srivastava *et al.* (1992a, 1992b) and the CC(2) calculations are due to Fabrikant (1980). Measurements are by Wang *et al.* (1994) and Jensen *et al.* (1978).

and excitations of the $(6s6p)^1P_1^o$ and $(6s5d)^1D_2^o$ states at 20 eV (Jensen *et al.* 1978; Wang *et al.* 1994). Our CCC(115) results are in essentially quantitative agreement with the experimental data for all three transitions presented and over all scattering angles. This is not the case for other theoretical methods. The CC(2) calculations of Fabrikant (1980) [elastic and $(6s6p)^1P_1^o$ DCS] are in fair agreement with experiment and our calculations at small scattering angles, but not at larger scattering angles. The UDWA calculations (Clark *et al.* 1989) and RDWA calculations (Srivastava 1992*a*, 1992*b*) are in poor agreement with experimental data [$(6s5d)^1D_2^o$ and $(6s6p)^1P_1^o$ DCS] at this incident electron energy, which is outside of the validity range of these distorted-wave approximation based methods.

Measurements of the EICPs for the $(6s6p)^1P_1^o$ state have been performed using the superelastic technique by Zetner *et al.* (1992, 1993) and Li and Zetner (1994).

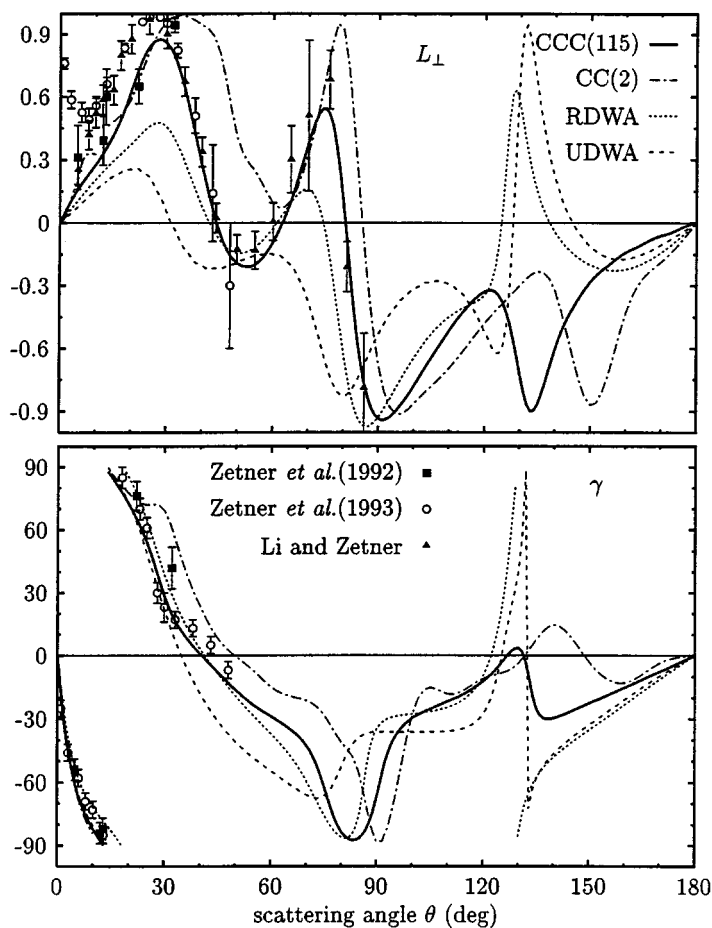


Fig. 3. EICPs L_{\perp} and γ of the $6s6p^1P_1^o$ state for electron scattering on the Ba ground state at 20 eV. Theoretical calculations are as for Fig. 2. Measurements are by Zetner *et al.* (1992, 1993) and Li and Zetner (1994).

This subject has been reviewed in a number of publications, see e.g. Andersen *et al.* (1988) and Slevin and Chwirot (1990) We refer to these references for the details and definitions of the EICPs L_{\perp} , γ and their relation to the Stokes parameters P_1 , P_2 and P_3 . Results of the CCC(115) calculations for L_{\perp} and γ are compared with experimental data and the results of other calculations in Fig. 3. We find that the CCC(115) results are in substantially better agreement with experiment than the earlier CC(2), UDWA and RDWA calculations, though some discrepancies in the case of L_{\perp} at small scattering angles have not been completely resolved. Below 30° there are also some discrepancies between different sets of measurements with our results favouring the data of Zetner *et al.* (1992).

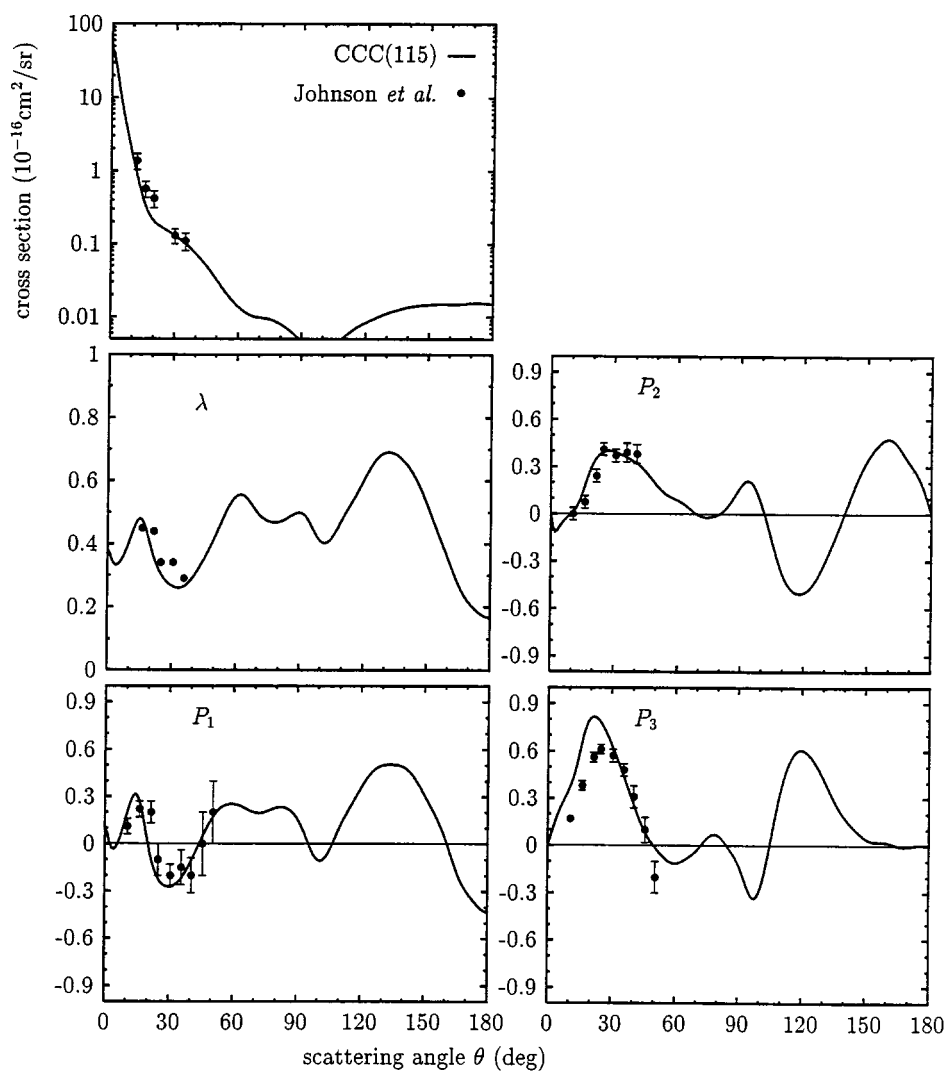


Fig. 4. Differential cross section and Stokes parameters P_1, P_2, P_3 and the parameter λ for electron impact excitation of the $6s6p^1P_1^o$ state from the $6s5d^1D_2^o$ state of barium at 10 eV. The CCC(115) calculation is described in the text. Measurements are by Johnson *et al.* (1990).

The effect of a finite scattering volume as discussed by Zetner *et al.* (1990) could influence some experimental data at small angles.

Having established a very good agreement between the CCC calculations and experiment for scattering from the barium ground state, we now turn to a comparison with experimental data for scattering from barium excited states. In Fig. 4 we present theoretical and experimental results for excitation of the $(6s6p)^1P_1^o$ state by electron impact from the isotropic $(6s5d)^1D_2^o$ level at 10 eV. DCS and Stokes parameters and the parameter λ for this transition have been measured by Johnson *et al.* (1999) using the superelastic technique, as has been discussed in the previous section. Agreement between theory and experiment is rather good. This is particularly encouraging because the $(6s5d)^1D_2^o-(6s6p)^1P_1^o$ transition is weak, which is consistent with the very small value of the optical oscillator strength for this transition.

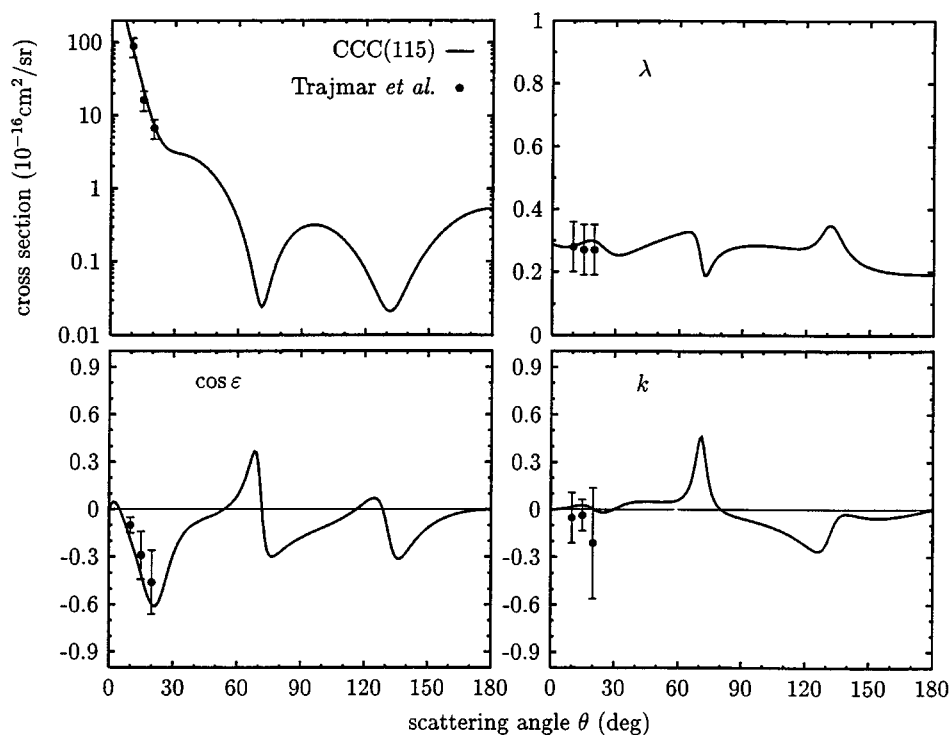


Fig. 5. Differential cross section and coherence parameters $\cos \varepsilon$, k and the parameter λ for e-Ba elastic scattering on the $6s6p^1P_1^o$ state at 20 eV. The CCC(115) calculation is described in the text. Measurements are by Trajmar *et al.* (1999).

We have found similarly good agreement between the CCC calculations and measurements of the DCS and coherence parameters $\cos \varepsilon$, k and the parameter λ (Trajmar *et al.* 1999) for e-Ba elastic scattering on the $6s6p^1P_1^o$ state at 20 eV (see Fig. 5). We refer to Trajmar *et al.* for a detailed discussion. The relation of the above coherence parameters to the Stokes parameters and EICPs can be found in Andersen *et al.* (1988).

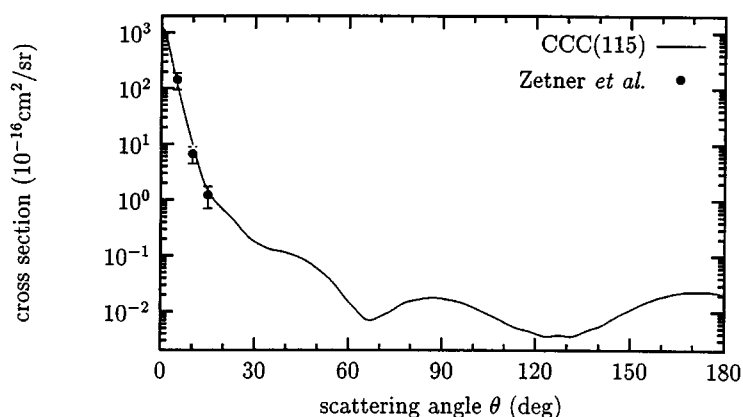


Fig. 6. Differential cross section for electron scattering from the $6s6p^1P_1^o$ to the $6s6d^1D_2^o$ state of barium at 20 eV. Experimental data are by Zetner *et al.* (1997).

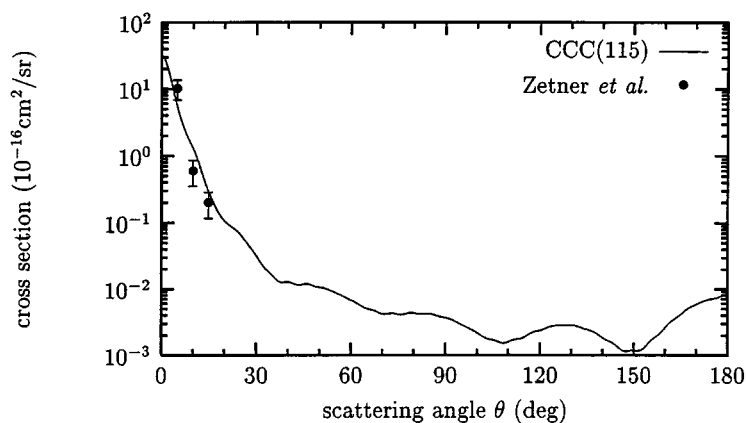


Fig. 7. Differential cross section for electron scattering from the $6s6p^1P_1^o$ to the $6s8p^1P_1^o$ state of barium (Moore's label: $6s7p^1P_1^o$) at 20 eV. Experimental data are by Zetner *et al.* (1997).

In Figs 6 and 7 we compare CCC results with measurements (Zetner *et al.* 1997) of the PDCS for the excitation of the $6s6d^1D_2^o$ and $6s8p^1P_1^o$ state at 20 eV from the laser-prepared $6s6p^1P_1^o$ state. Note that the latter state was labeled $6s7p^1P_1^o$ by Moore (1949). Linearly polarised laser light propagating in the scattering plane has been used, which corresponds to the following choice of the angles in equation (22): $\theta_\nu = 45^\circ$, $\varphi = 0^\circ$ and $\psi = 54.7^\circ$. Agreement with experiment is very good for both transitions.

Finally we would like to present a comparison with experimental data (Zetner *et al.* (1999) for scattering from the $6s5d^1D_2^o$ and $6s5d^3D_2^o$ metastable levels. Results for the $6s7p^1P_1^o$ – $6s5d^1D_2^o$ and $6p5d^3P_{0,1,2}$ – $6s5d^3D_2^o$ transitions are presented in Figs 8 and 9 respectively. Note that the $6s7p^1P_1^o$ state has been labeled as $6p5d^1P_1^o$ by Moore (1949). Experimental analysis has shown that the

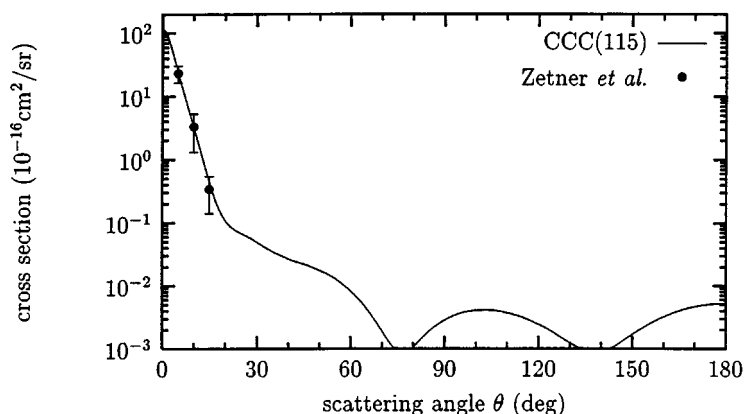


Fig. 8. Differential cross section for electron scattering from the $6s5d^1D_2^o$ to the $6s7p^1P_1^o$ state of barium (Moore's label: $6p5d^1P_1^o$) at 20 eV. Experimental data are by Zetner *et al.* (1999).

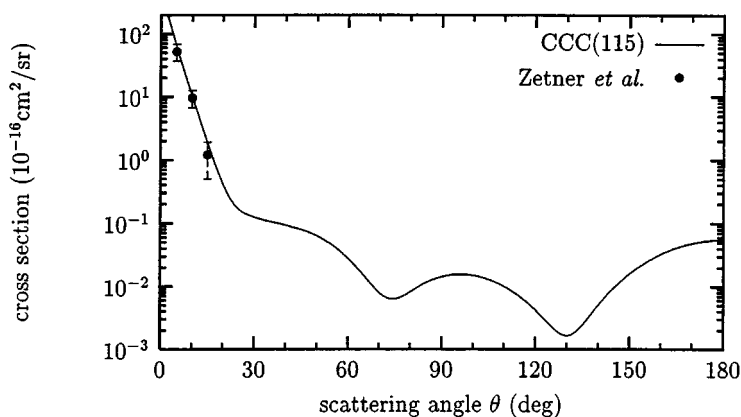


Fig. 9. Differential cross section for electron scattering from $6s5d^3D_2^o$ to the $6p5d^3P_{1,2}^o$ states of barium at 20 eV. Experimental data are by Zetner *et al.* (1999).

population of the metastable levels is essentially isotropic, which might be caused by the radiation trapping effect. We, therefore, present CCC differential cross sections for scattering from an isotropic initial state. These CCC results are found to be in excellent agreement with experimental data.

5. Conclusions

We have presented some results of a joint experimental and theoretical program concerning electron scattering from the barium atom. The theoretical method we have used in this study is the CCC method. We have demonstrated the applicability of the CCC method to describe e-Ba scattering from the ground state and have shown very good quantitative agreement with the accurate experimental data available.

Electron scattering from the barium atom excited states has been studied for the laser-excited $6s6p^1P_1^o$ level and the cascade-populated metastable $6s5d^1,^3D_2^o$ levels. Experimental measurements have been performed for a wide range of scattering processes which included differential cross sections and EICPs. Good agreement has been found between CCC results and experimental data.

Acknowledgments

Support of the Australian Research Council and the Flinders University of South Australia is acknowledged. We are also indebted to the South Australian Centre for High Performance Computing and Communications.

References

- Andersen, N., Gallagher, J. W., and Hertel, I. V. (1988). *Phys. Rep.* **165**, 1.
- Bauschlicher, Jr, C. W., Jaffe, R. L., Langhoff, Y., Mascarello, F. G., and Partridge, H. (1985). *J. Phys. B* **18**, 2147.
- Bizzarri, A., and Huber, M. C. E. (1990). *Phys. Rev. A* **42**, 5422.
- Bray, I. (1994). *Phys. Rev. A* **49**, 1066.
- Bray, I., and Stelbovics, A. T. (1992). *Phys. Rev. A* **46**, 6995.
- Chen, S. T., and Gallagher, A. (1976). *Phys. Rev. A* **14**, 593.
- Chernysheva, L. V., Cherepkov, N. A., and Radojevic, V. (1976). *Comput. Phys. Commun.* **11**, 57.
- Clark, R. E., Abdallah, Jr, J., Csanak, G., and Kramer, S. P. (1989). *Phys. Rev. A* **40**, 2935.
- da Paixão, F. J., Padial, N. T., Csanak, G., and Blum, K. (1980). *Phys. Rev. Lett.* **345**, 1164.
- Dettmann, J., and Karstensen, F. (1982). *J. Phys. B* **15**, 287.
- Edmonds, A. R. (1957). 'Angular Momentum in Quantum Mechanics' (Princeton Univ. Press).
- Fabrikant, I. I. (1980). *J. Phys. B* **13**, 603.
- Fursa, D. V., and Bray, I. (1995). *Phys. Rev. A* **52**, 1279.
- Fursa, D. V., and Bray, I. (1997). *J. Phys. B* **30**, 5895.
- Fursa, D. V., and Bray, I. (1999). *Phys. Rev. A* **59**, 282.
- Jensen, S., Register, D., and Trajmar, S. (1978). *J. Phys. B* **11**, 2367.
- Johnson, P. V., Eves, B., Zetner, P. W., Fursa, D. V., and Bray, I. (1999). *Phys. Rev. A* **59**, 439.
- Karaganov, V., Bray, I., Teubner, P. J. O., and Farrell, P. (1996). *Phys. Rev. A* **54**, R9.
- Korenman, G. Y. (1975). *Sov. J. Nucl. Phys.* **21**, 398.
- Li, Y., and Zetner, P. W. (1994). *Phys. Rev. A* **49**, 950.
- Li, Y., and Zetner, P. W. (1995). *J. Phys. B* **28**, 5151.
- Macek, J., and Hertel, I. V. (1974). *J. Phys. B* **7**, 2173.
- Moore, C. E. (1949). 'Atomic Energy Levels', Circ. No. 467, Vol. III (NBS: Washington, DC).
- Romanyuk, N. I., Spornik, O. B., and Zapesochny, I. P. (1980). *JETP Lett.* **32**, 452.
- Rose, S. J., Pyper, N. C., and Grant, I. P. (1978). *J. Phys. B* **5**, 755.
- Slevin, J. A., and Chwirot, S. (1990). *J. Phys. B* **23**, 165.
- Srivastava, R., McEachran, R. P., and Stauffer, A. D. (1992a). *J. Phys. B* **25**, 4033.
- Srivastava, R., Zuo, T., McEachran, R. P., and Stauffer, A. D. (1992b). *Phys. Rev. B* **25**, 3709.
- Trajmar, S., Kanik, I., Khakoo, M. A., LeClair, L., Bray, I., Fursa, D. V., and Csanak, G. (1998). *J. Phys. B* **31**, L393.
- Trajmar, S., Kanik, I., Khakoo, M. A., LeClair, L., Bray, I., Fursa, D. V., and Csanak, G. (1999). *J. Phys. B*, to be published.
- Treffitz, E. (1974). *J. Phys. B* **7**, L342.
- Wang, S., Trajmar, S., and Zetner, P. W. (1994). *J. Phys. B* **27**, 1613.
- Zetner, P. W., Li, Y., and Trajmar, S. (1992). *J. Phys. B* **25**, 3187.
- Zetner, P. W., Li, Y., and Trajmar, S. (1993). *Phys. Rev. A* **48**, 495.
- Zetner, P. W., Trajmar, S., and Csanak, G. (1990). *Phys. Rev. A* **41**, 5980.
- Zetner, P. W., Trajmar, S., Kanik, I., Wang, S., Csanak, G., Clark, R. E. H., and Abdallah, Jr, J. A., Fursa, D. V., and Bray, I. (1999). *J. Phys. B*, to be published.
- Zetner, P. W., Trajmar, S., Wang, S., Kanik, I., Csanak, G., Clark, R. E., Abdallah, Jr, J. A., and Nickel, J. C. (1997). *J. Phys. B* **30**, 5317.